

Nonlinear Multi-wavelength Conversion Based on Aperiodic Optical Superlattice in Lithium Niobate

Y.W. Lee¹, F. C. Fan¹, B. Y. Gu², B. Z. Dong², M. H. Chou³ and Y. C. Huang¹

¹Department of Electrical Engineering, National Tsinghua University, Hsinchu 300, Taiwan

²Institute of Physics, Chinese Academy of Sciences, P.O.Box 603, Beijing 100080, P.R. China.

³Tellium Inc., 2 Crescent Place, P.O.Box 901, Oceanport, NJ 07757-0901, U.S.A.

Abstract: We have demonstrated the first successful experiment of multi-wavelength conversion in an aperiodic-optical-superlattice (AOS) lithium niobate crystal with equalized gain. Our experiment and simulation show that the output spectrum of an AOS wavelength converter is insensitive to typical fabrication errors.

©2002 Optical Society of America

OCIS codes: (190.2620) Nonlinear Optics, frequency conversion; (190.4360) Nonlinear Optics, devices

1. Introduction

In the past few decades, nonlinear optics has been exploited extensively to vary the wavelength of an existing laser source. Due to the phase-matching requirement in the nonlinear process, birefringence nonlinear optical crystals are often the chosen materials for nonlinear frequency conversion. To access a large nonlinear coefficient without being restricted by the birefringence of a nonlinear crystal, the quasi-phase-matching (QPM) technique has been proposed [1] and demonstrated [2] as an efficient means for nonlinear frequency conversion. One of the attractive applications is to design the QPM nonlinear crystal for obtaining a device with multiple-phase-matching wavelengths. For example, Zhu et al. used the Fibonacci optical superlattice (FOS) in lithium niobate to generate multiple second-harmonic-generation (SHG) wavelengths [3]; however, the FOS technique appears to be very sensitive to fabrication errors and difficult to achieve the designed spectrum [4]. Chou et al. implemented the phase-reversal-sequence (PRS) technique on the periodically poled lithium niobate (PPLN) waveguide [5]; however, unwanted side bands often show up in the PRS output spectrum and could cause, for example, cross-talk in communication applications.

2. Theory

The concept of AOS nonlinear wavelength conversion is to ensure simultaneous coherence gain enhancement for all output wavelengths in a nonlinear crystal. The AOS technique adopts the so-called simulated annealing (SA) method to optimize the conversion efficiency for each design wavelength [4,6]. There are two major factors contributing to an AOS output spectrum. One factor is the length of a unit crystal block, which must be shorter than any of the coherence lengths in the wave mixing process. The other factor is the proper arrangement of the polarizations of those crystal blocks, which ensures all the converted waves to grow coherently. Figure 1.(a) shows the schematic plot of a typical AOS wavelength converter. The AOS device consists of nonlinear crystal blocks with each having a length of dx . Adjacent crystal blocks may have the same or the opposite nonlinear polarization direction. The choice of the polarization direction is determined by the SA algorithm. Figure 1.(a) also labels the ideal boundary position of the q th crystal block as x_q and non-ideal boundary position as x'_q . The non-ideal boundary position may result from some typical but uncontrollable fabrication process.

The SHG conversion efficiency η_{SHG} in an AOS nonlinear crystal having N crystal blocks along the x direction is given by [6],

$$(1) \quad \eta_{SHG}(\lambda) = \eta_{eff}(\lambda) \times \left| \sum_{q=0}^{N-1} \int_{x'_q}^{x'_{q+1}} \tilde{d}_q e^{i\Delta k x} dx \right|^2$$

where c is the fundamental laser wavelength in a vacuum, $\eta_{eff}(\lambda)$ is the normalized efficiency defined below, the nonlinear polarization \tilde{d}_q takes the binary value of 1 or -1 for the q th crystal block between x'_q and x'_{q+1} , and Δk is the wave vector mismatch between the fundamental and the second harmonic waves. For lithium niobate with all mixing waves polarized in the crystallographic c direction, the normalized efficiency is given by

$$\eta_{\text{eff}}(\lambda) = \frac{8\pi^2 |d_{33}|^2 I_\omega}{c \varepsilon_0 \lambda^2 n_{2\omega} n_\omega^2} \quad (2)$$

where c is the vacuum wave speed, ε_0 is the vacuum permittivity, d_{33} is the nonlinear coefficient, and I_ω is the laser intensity of the fundamental wave, and $n_{\omega, 2\omega}$ represent the refractive indices of the fundamental and the second harmonic wave with the angular frequency ω and 2ω , respectively. With a specified crystal block length and some gain weighting factors, the SA code starts to maximize Eq. (1) at all design wavelengths by calculating their conversion efficiencies while synthesizing the crystal blocks one by one with the proper choice of \tilde{d}_q .

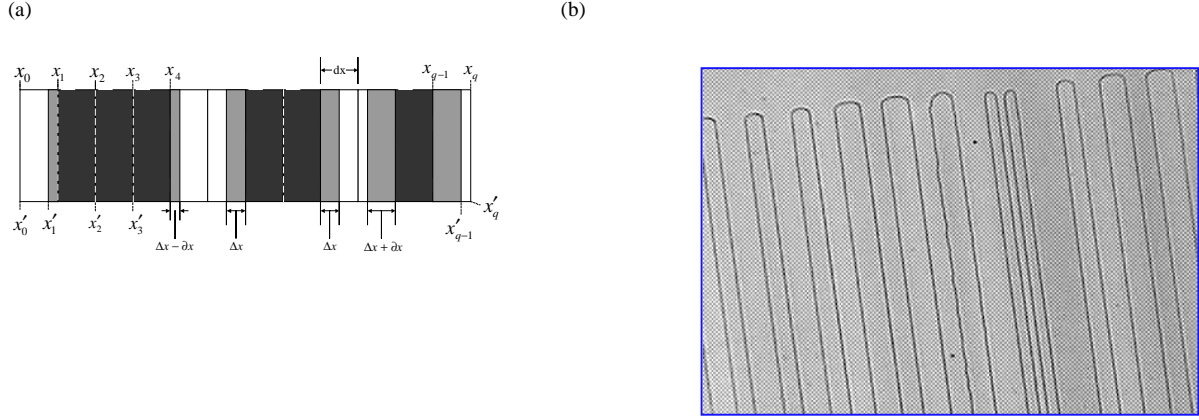


Fig. 1. (a) The schematic plot of an AOS crystal, wherein x_q is the q th crystal boundary of an ideal AOS crystal, and dx is the length of a unit crystal block. With fabrication errors, x'_q is q th crystal boundary position, Δx is the uniformly over-poled domain length, and ∂x is the random variation in Δx . (b) A typical section of the HF etched AOS crystal used in our experiment. The unit crystal block length dx is $3.5 \mu\text{m}$.

3. Experiment

To fabricate the AOS lithium niobate, we adopted the conventional lithographic and electric-field poling technique for PPLN with a modified transmission pattern on the photo-mask. We fabricated a double-wavelength AOS device and a triple-wavelength AOS device according to our simulation results. Both AOS devices have a unit crystal length of $3.5 \mu\text{m}$ and a total length of 1-cm. In the SHG experiment, the pump source was a continuous-wave external-cavity diode laser followed by an Erbium-doped fiber amplifier. The pump wavelength can be tuned from 1530 nm to 1560 nm with approximately 26-mW pump power. A 20-mm focal-length lens focused the pump beam to the center of the AOS lithium niobate. The fundamental wavelengths for the double-wavelength AOS SHG are 1540 nm and 1545 nm, and those for the triple-wavelength AOS SHG are 1540 nm, 1545 nm, and 1553 nm. To compare, we also fabricated an $18.9 \mu\text{m}$ -period PPLN of the same length phase-matched to the SHG of the 1540 nm fundamental wavelength. Figures 2.(a,b) are the output spectra of the double and triple-wavelength SHG. The horizontal axes are labeled with the fundamental wavelength and the vertical axes are normalized to the single-wavelength SHG conversion efficiency from the $18.9 \mu\text{m}$ -period PPLN. For the double-wavelength and the triple-wavelength AOS SHG, the peak efficiencies normalized to the PPLN are 38% and ~25%, respectively. In Figs.2, there is little difference between the experimental results (solid dots) and the simulation predictions (continuous curves). The inset in Fig. 2.(b) shows the calculation of the triple-wavelength PRS SHG spectrum, which has significantly more side-band power and less conversion efficiency when compared with those for the triple-wavelength AOS SHG. The AOS technique has the flexibility of choosing an arbitrarily small crystal block for crystal synthesis and its output spectrum can be greatly optimized.

Reference [4] has shown that the SHG output spectrum of an AOS device could be seriously distorted by a merely 3% random error in each crystal block length. Although we estimated an average over-poled error of $\Delta x/dx \approx 7\%$ and a random error of $|\delta x/dx| \leq 4\%$ along our triple-wavelength AOS crystal, the measured triple-wavelength SHG spectrum in Fig. 2.(b) agreed surprisingly well with our simulation. Figure 3 shows the simulation result for the AOS crystal having random domain errors of $|\partial x/dx| \leq 20\%$ and $|\partial x/dx| \leq 30\%$ under a uniformly over-poled average error of $\Delta x/dx = 20\%$ based on the $3.5 \mu\text{m}$ unit block length. It is seen from the plot

that the SHG efficiency is very insensitive to the fabrication errors as observed in our experiment. The reason is that the AOS output spectrum is the Fourier transform of the AOS pattern on the photo-mask, which is imaged directly to the nonlinear crystal through the lithographic process.

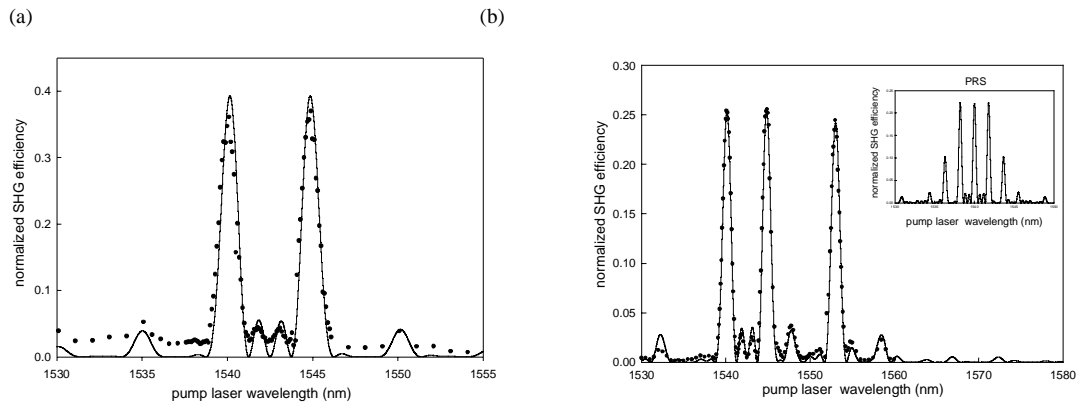


Fig 2. The experimental (shown by solid dots) and theoretical (shown by curves) conversion efficiencies of the (a) double-wavelength and (b) triple-wavelength AOS SHG. The vertical axes are normalized to the peak SHG conversion efficiency of the 18.9 μm -period SHG PPLN, and the horizontal axes are the fundamental wavelength. The inset in (b) shows the output spectrum of triple-wavelength PRS SHG, in which the peak conversion efficiency is lower and side-band power is higher.

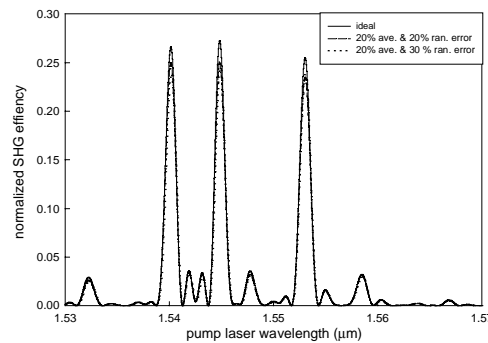


Fig. 3. The simulation result for the AOS crystal having random domain errors of $|\partial x / \partial x| \leq 20\%$ and $|\partial x / \partial x| \leq 30\%$ under a uniformly over-poled average error of $\Delta x / dx = 20\%$. The AOS output spectrum is not sensitive to fabrication errors.

4. Conclusions

In conclusion, we have demonstrated the first successful AOS device for nonlinear multi-wavelength conversion. The measured SHG spectra are in good agreement with our design. We have also simulated the effect of typical fabrication errors to an AOS device and found that an AOS wavelength converter is fairly insensitive to the errors. The AOS has the ability of incorporating pump depletion into computer simulation. In the future, we will be investigating the performance of a high-efficiency nonlinear AOS waveguide, in which pump depletion often occurs.

References:

- [1]. J. A. Armstrong, N. Bloembergen, J. Ducuing, and P. S. Perhan, Phys. Rev. Lett. **127**, 1918-1939 (1962).
- [2]. L. E. Myers, R. C. Eckardt, M.M. Fejer, R.L. Byer, W. R. Bosenberg, J. W. Pierce, J. Opt. Soc. Am. B **12**, 2102-2116 (1995).
- [3]. M. A. Arbore, O. Marco, M. M. Fejer, Opt. Lett. **22**, 865-867 (1997).
- [4]. G. Imeshev, A. Galvanauskas, D. Harter, M. A. Arboer, M. Proctor, and M. M. Fejer, Opt. Lett. **23**, 864-866 (1998).
- [5]. S. N. Zhu, Y. Y. Zhu and N. B. Ming, Science **278**, 843-852, (1997)
- [6]. Ben-Yuan Gu, Yan Zhang and Bi-Zhen Dong, Journal of Applied physics, **87**, 7629-7637 (2000).
- [7]. M. H. Chou, K. R. Parameswaran, and M. M. Fejer, Opt. Lett. **24**, 1157-1159 (1999).
- [8]. Ben-Yuan Gu, Bi-Zhen Dong, Yan Zhang and Guo-Zhen Yang, Applied Physics Letters, **75**, 2175-2177 (1999).